



## A bi-layer electrospun nanofiber membrane for plasmid DNA recovery from fermentation broths

Tiago R. Correia<sup>a</sup>, Bernardo P. Antunes<sup>a</sup>, Pedro H. Castilho<sup>a</sup>, José C. Nunes<sup>a</sup>, Maria T. Pessoa de Amorim<sup>b</sup>, Isabel C. Escobar<sup>c</sup>, João A. Queiroz<sup>a</sup>, Ilídio J. Correia<sup>a,\*</sup>, António M. Morão<sup>a</sup>

<sup>a</sup> CICS-UBI – Health Sciences Research Center, Faculty of Health Sciences, University of Beira Interior, Covilhã, Portugal

<sup>b</sup> Department of Textile Engineering, University of Minho, 4800-058 Guimarães, Portugal

<sup>c</sup> Department of Chemical and Environmental Engineering, University of Toledo, Toledo, OH 43606, United States

### ARTICLE INFO

#### Article history:

Received 2 February 2013

Received in revised form 28 March 2013

Accepted 29 March 2013

Available online 6 April 2013

#### Keywords:

Microfiltration  
Electrospinning  
Bi-layer membrane  
Lysate  
Plasmid DNA

### ABSTRACT

The demanding ever-increasing quantities of highly purified biomolecules by bio-industries, has triggered the development of new, more efficient, purification techniques. The application of membrane-based technologies has become very attractive in this field, for their high throughput capability, simplicity of operation and scale-up.

Herein we report the production of a bi-layer membrane by electrospinning (ES), in which a support of poly  $\epsilon$ -caprolactone nanofibers was coated with a polyethylene oxide/sodium alginate layer, and subsequently cross-linked with calcium chloride. The membranes were characterized by SEM, ATR-FTIR, contact angle measurements, and were applied in the recovery process of a plasmid. The results show that membranes retained the suspended solids while allowing the permeation of plasmid DNA, with high recovery yields and improved RNA retention. Moreover, they also showed a very low fouling tendency. To the best of our knowledge it is the first time that ES membranes are applied in this type of bioprocess.

© 2013 Elsevier B.V. All rights reserved.

### 1. Introduction

The development of new separation technologies suitable for the large-scale production of highly purified plasmid DNA (pDNA) for gene therapy applications and the production of DNA vaccines has found increasing interest in the recent years [1–4]. The use of microfiltration and ultrafiltration membranes for pDNA recovery and purification from fermentation broths has been demonstrated as a promising alternative to conventional separation methods, namely those involving precipitation with solvents and centrifugation [5].

Electrospinning is an easy and cheap method of producing nanofibrous materials. These can be obtained from a wide variety of polymers by controlling the solution properties and the processing conditions [6]. The simplicity of this procedure and the wide range of applications found in recent years, including tissue engineering applications, such as bone repair, wound healing and drug delivery carriers [7–9], in sensors and biosensors [10], in electrodes [11] and that of filtration [12–14] are important factors that lead to an increasing interest in developing new types of electrospun nanofiber membranes (ENMs) [15]. Commonly, nanofibers

are electrospun into a support or produced in layer by layer arrangements [16,17]. In either case fiber deposition should be always carried out on a support which provides the required mechanical strength to the films produced [16].

In the present study, a poly  $\epsilon$ -caprolactone (PCL) support was prepared by a conventional electrospinning process. This polymer was selected based on the good mechanical properties that PCL meshes present [18] and also for being environmentally friendly [19]. A coating based on an electrospun mixture of two polymers, sodium alginate (SA) combined with poly(ethylene) oxide (PEO) was deposited on the support. SA was selected for ENMs coating due to its high hydrophilicity, relatively low cost and the ability of producing small diameter fibers by electrospinning, when mixed with PEO [20]. This asymmetric arrangement of two different layers provides the membrane with adequate mechanical robustness whereas separation selectiveness is regulated predominantly by the ultrathin layer of nanofibers.

The bi-layer membranes produced were characterized in terms of their morphology, hydrophilicity and hydraulic permeability prior to the filtration tests. The performance of the ENMs on the filtration of cell lysates, obtained immediately after the cell lysis step, was evaluated and compared with that of commercial microfiltration membranes. From the best of our knowledge, this is the first time that ENMs are tested in the recovery process of biomolecules from fermentation broths.

\* Corresponding author. Address: Av. Infante D. Henrique, 6200-506 Covilhã, Portugal. Tel.: +351 275 329 002; fax: +351 275 329 099.

E-mail address: [icorreia@ubi.pt](mailto:icorreia@ubi.pt) (I.J. Correia).

## 2. Materials and methods

### 2.1. Materials

PEO (Mw = 300,000 g/mol), SA (Mw = 120,000–190,000 g/mol), PCL (Mw = 80,000 g/mol), calcium chloride (Mw = 110.99 g/mol) were purchased from Sigma–Aldrich (Sin tra, Portugal) as well as Terrific Broth medium for bacterial culture and kanamycin sulfate. P1 buffer (50 mM Tris–HCl, pH = 8.00, 10 mM EDTA and 100 µg/mL of RNase A), P2 buffer (200 mM NaOH and 1% SDS (w/v)) and P3 buffer (3 M of potassium acetate, pH 5.00) were from a Qiagen Plasmid Maxi Kit and Tris–HCl 10 mM (IZASA, Portugal). Microfiltration membranes, *Nyloflo* (pore diameter of 0.22 µm *Pall Corporation* and *FSM0.45PP* from *Alfa Laval* (pore diameter of 0.45 µm).

### 2.2. Methods

#### 2.2.1. Bacterial growth and cell lysis

The plasmid production procedure was adapted from the literature [5,21]. The 6050 bp plasmid pVAX1-LacZ was amplified in a cell culture of *Escherichia coli* DH5α. The fermentation was carried out at 37 °C in 250 mL of Terrific Broth medium, supplemented with 50 µg/mL of kanamycin. Growth was suspended at the late log phase ( $OD_{600\text{nm}} \approx 10\text{--}11$ ) and cells were harvested by centrifugation. Afterwards, pDNA extraction was performed by alkaline lysis using three different buffers (P1, P2 and P3, previously specified). For this procedure 120 g/L (wet weight) of cells were resuspended in 4 mL of P1 buffer. Then, 4 mL of P2 were added to promote cell lysis for 5 min, at room temperature. Finally, P3 buffer at 4 °C was added to neutralize the alkaline solution. A large quantity of suspended solids was obtained upon neutralization and the suspension was kept on ice for 15 min before membrane filtration.

#### 2.2.2. ENMs production process

A conventional electrospinning apparatus was used for ENMs production. The system setup consisted in a high voltage source (*Spellman CZE1000R*, 0–30 kV), a syringe pump (*KDS-100*), a plastic syringe with a stainless steel needle and an aluminum disk connected to a copper collector. PCL was dissolved in acetone (10% w/v), at 50 °C, under constant stirring [22]. Meanwhile, a PEO/SA solution was prepared by mixing 6.75% PEO and 0.5% SA aqueous solutions [23]. The PCL polymer solution was used to produce a support ENM, using a constant flow rate of 3 mL/h and an applied voltage of 15 kV. The distance between needle tip and collector was set at 10 cm [22]. Subsequently, the PEO/SA solution was deposited over the PCL ENM by electrospinning, in the same apparatus, at a constant flow rate of 0.6 mL/h and an applied voltage of 18 kV, thereby obtaining a bi-layer ENM. Finally, the

membrane was crosslinked in a calcium chloride solution for 24 h [23]. From the obtained films, membranes disks were cut with suitable size to be used in the filtration cell, using a circular blade.

#### 2.2.3. Membrane filtration tests

These assays were performed in a 10 mL stirred cell (*Amicon/Millipore*, model 8010), according to a procedure previously described in the literature [19]. The membranes to be tested (*Nyloflo*, *FSM0.45PP* or the ENMs) were initially flushed with 20 mL of *Milli-Q* water at a constant pressure of 0.07 bar, to ensure the thorough washing of the membranes. Then, the water permeability (hydraulic permeability) of each membrane was determined by measuring the flow rate, at that pressure. Five permeability measurements were performed with each membrane disk and the average value was considered the initial hydraulic permeability of each membrane disk,  $L_{p0}$ .

To perform the filtration of the *E. coli* DH5α lysates the remaining water in the cell was carefully removed and, immediately after that, 10 mL of lysate were introduced in the filtration cell. A continuous diafiltration of the lysate was performed for 1 h, using a 10 mM Tris–HCl (pH = 8.00) buffer at a constant flow rate of 0.5 mL/min. Two peristaltic pumps were used, one for feeding the diafiltration buffer and the other to perform the filtration (by suction). The experimental setup is shown in Fig. 1. Under these conditions, one could estimate that, if no pDNA was adsorbed on the membrane and the membrane rejection was 0, approximately 95% of the pDNA was expected to be recovered in the permeate, while 5% would remain in the cell. It was decided to not try to recover the remaining pDNA to avoid excessive dilution of the whole permeate.

#### 2.2.4. Turbidity measurements

The filtrate was analyzed by UV/Visible Spectroscopy at a wavelength of 600 nm, to determine the amount of suspended solids. A fraction of the alkaline lysate, containing the suspended solids, was transferred to an eppendorf tube and centrifuged at 18,000g during 30 min at 4 °C (*Hettich Zentrifugen, Mikro 200R*). Then, the absorbance of the supernatant was measured at a wavelength of 600 nm and the value obtained compared with that of the membrane permeates.

#### 2.2.5. Plasmid DNA and RNA quantification

Plasmid DNA and RNA concentrations in lysates, were obtained by hydrophobic interaction chromatography (HIC) [5]. Briefly, a 15 PHE PE column (*Amersham Biosciences – GE Healthcare*) connected to an AKTA purifier HPLC System was used. The column was initially equilibrated with 1.5 M  $(\text{NH}_4)_2\text{SO}_4$  in a 10 mM Tris–HCl buffer (pH 8.00). Prior to the injection, the suspended solids in lysates were removed by centrifugation, as described in Section 2.2.4.

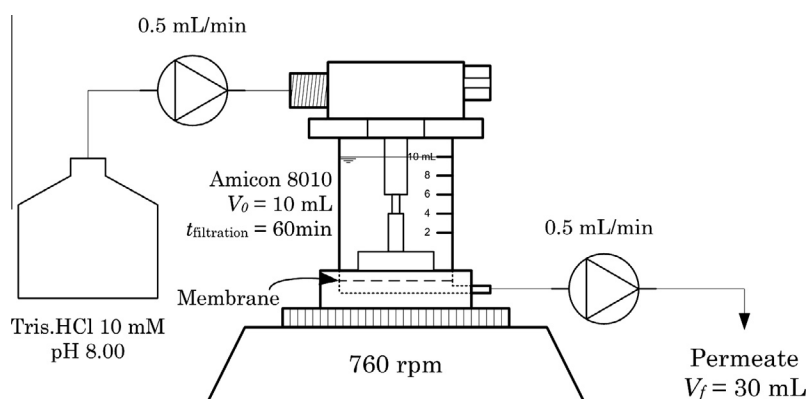


Fig. 1. Experimental set-up used for continuous diafiltrations, showing the two peristaltic pumps and the filtration cell.

Samples from the supernatants were directly injected in the column. The injected volume in each run was 20  $\mu\text{L}$  and the samples were eluted at a constant flow rate of 1 mL/min. Two minutes after the injection, the eluent was instantly changed to 10 mM Tris–HCl buffer (pH = 8.00), in order to elute bounded species. This concentration was maintained for 5 min before the re-equilibration of the column, which was carried out with 1.5 M  $(\text{NH}_4)_2\text{SO}_4$  in a 10 mM Tris–HCl buffer (pH 8.00), in order to prepare the column for the next run. The absorbance of the eluate at 260 nm was monitored. The concentration of pDNA in each sample was calculated from the area of the pDNA peak and a calibration curve, obtained with pure pVAX1-lacZ standard solutions.

The filtration yield, in each test, was calculated as the ratio of the amount of pDNA in the whole collected permeate to the amount of pDNA in the lysate. The RNA removal was calculated as  $1 - (V_p C_{RNA,p}) / (V_{lys} C_{RNA,lys})$  where  $C_{RNA,p}$  is the RNA concentration in the whole collected permeate and  $C_{RNA,lys}$  is the RNA concentration in the lysate,  $V_p$  is the whole volume of permeate collected and  $V_{lys}$  is the volume of lysate processed in each run.

#### 2.2.6. Scanning electron microscopy

The morphology of the membranes was analyzed by scanning electron microscopy (SEM). Samples were air-dried overnight and then mounted on an aluminum board using a double-side adhesive tape and covered with gold using an *Emitech K550* (London, England) sputter coater. The samples were analyzed using a *Hitachi S-2700* (Tokyo, Japan) scanning electron microscope operated at an accelerating voltage of 20 kV and at different amplifications [21].

The diameter distribution of the nanofibers in the ENMs was determined from 50 measurements, at least, using *ImageJ* (National Institutes of Health, Bethesda (MD), USA).

#### 2.2.7. Attenuated total reflectance-fourier transform infrared spectroscopy

PEO, SA, PCL and polymer coated ENMs spectra were acquired in the range of 4000–500  $\text{cm}^{-1}$ , using a *JASCO 4200 FTIR* spectrophotometer, operating in ATR mode (*MKII GoldenGate™* Single Reflexion ATR System). Data collection was performed with a 4  $\text{cm}^{-1}$  spectral resolution and after 64 scans [24].

#### 2.2.8. Contact angle

Contact angles of the membranes were determined using a *Data Physics Contact Angle System OCAH 200* apparatus, operating in static mode. For each sample, water drops were placed at various locations of the analyzed surface, at room temperature. The reported contact angles are the average of at least three measurements.

#### 2.2.9. Membrane porosity

The surface porosity of the membranes was estimated from SEM images using the image analysis software, *ImageJ*. The total porosity of the membranes was measured through the determination of the amount of ethanol absorbed by wet membranes, after 1 h of immersion in that solvent, using the following equation [25]:

$$P(\%) = \frac{W_2 - W_1}{d_{\text{ethanol}} V_{\text{membrane}}} \times 100 \quad (1)$$

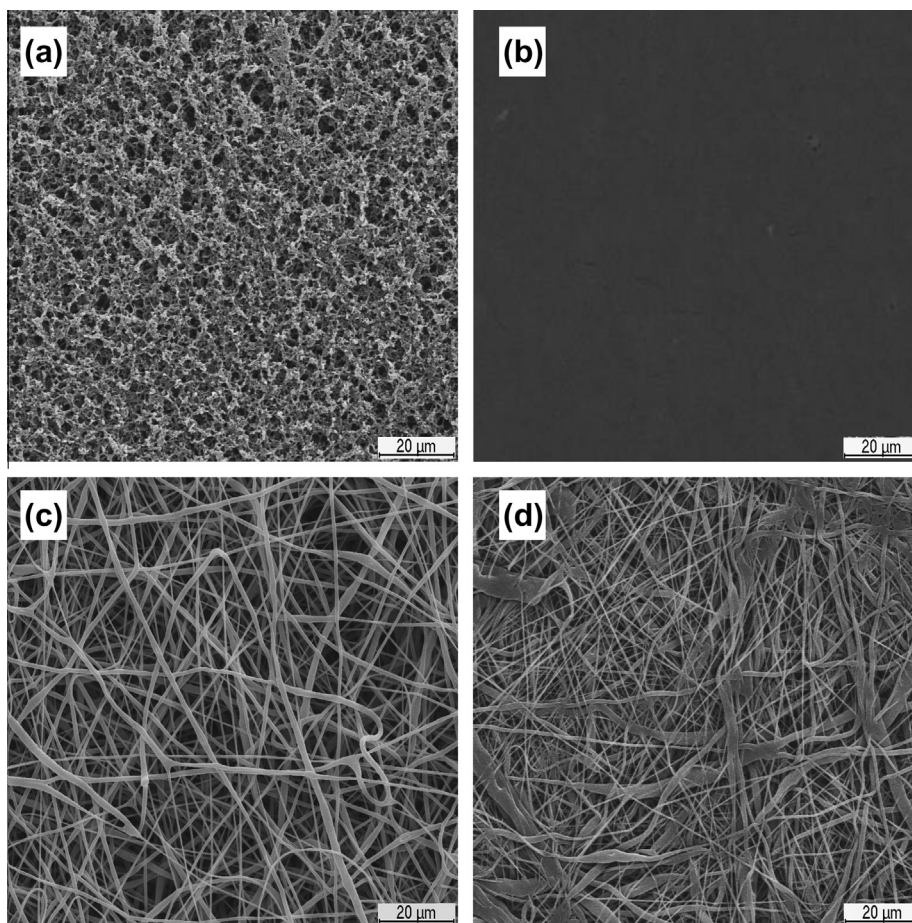


Fig. 2. SEM images. (a) Nylaflo 0.22  $\mu\text{m}$  membrane; (b) FSM0.45PP 0.45  $\mu\text{m}$  membrane; (c) PCL ENM; and (d) PCL ENMC.

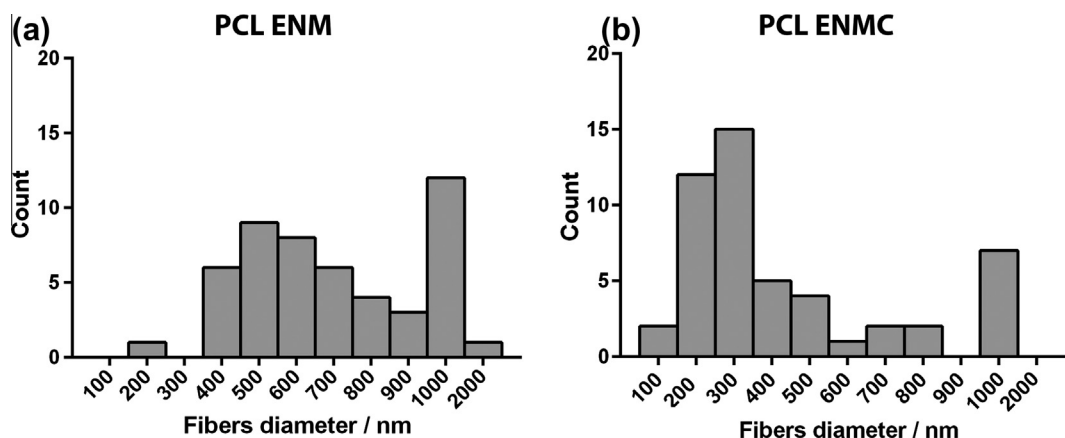


Fig. 3. Fiber diameter distribution for the uncoated and coated PCL ENM.

where  $W_1$  is the weight of the dry membrane and  $W_2$  is the weight of the wet membrane,  $d_{\text{ethanol}}$  the density of the ethanol at room temperature, and  $V_{\text{membrane}}$  is the volume of the wet membrane. The latter was determined from the membrane area and by measuring the membrane thickness with a micrometer *Adamel Lhomargy M120* acquired from *Testing Machines Inc., USA*.

### 3. Results and discussion

#### 3.1. ENMs characterization

The morphology of the membranes, namely in terms of fiber diameter distribution, fiber average diameter and surface porosity was analyzed from SEM images. As can be seen in Fig. 2 the ENMs produced present a high density of deposited fibers, in particular after deposition of the second layer of nanofibers.

Fiber diameter distributions are shown in Fig. 3. The PCL support has nanofibers with different diameters (200 nm – 2  $\mu\text{m}$ ) and this range of fiber diameters is adequate for obtaining a good mechanical support [26]. The polymer-coated ENM presents a higher density of thin fibers (i.e., fibers with 200–300 nm of diameter) than the polymer-uncoated ENM (i.e., the PCL support) which contributes to a decrease in the dimensions of the interstices. The number average fiber diameter of the uncoated ENMs can be estimated to be 720 nm and that of the coated membranes to be 430 nm. The commercial microfiltration membranes have typical values of pore diameter for this type of membranes, 0.22  $\mu\text{m}$  and 0.45  $\mu\text{m}$  for the *Nylaflo* and *FSM0.45PP*, respectively (nominal values given by the manufacturers).

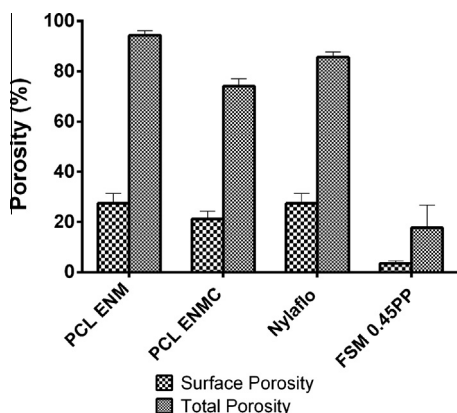


Fig. 4. Surface and total porosity of the ENMs and the commercial microfiltration membranes.

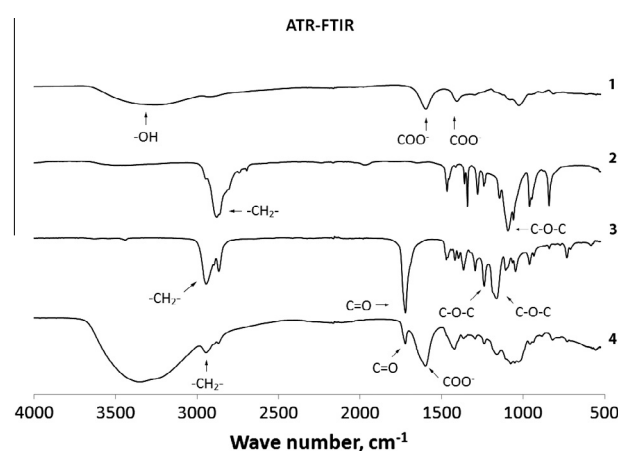


Fig. 5. ATR-FTIR spectra of: (1) SA; (2) PEO; (3) PCL ENM; and (4) PCL ENMC.

The porosity of the membranes is analyzed in Fig. 4. As can be seen, the ENMs have porosities comparable to that of the 0.22  $\mu\text{m}$  *Nylaflo* membranes which have been found to perform very satisfactory in the filtration of lysates from plasmid pVAX1-lacZ fermentation [5]. The porosity of the 0.45  $\mu\text{m}$  membrane used is clearly lower than that of the other membranes studied herein.

An ATR-FTIR analysis of the membranes was also carried out to check for the presence of the coating layer. The ATR-FTIR spectra of SA, PEO, PCL and the PCL/SA ENM (polymer coated ENM) can be seen in Fig. 5. The spectrum of SA shows its characteristic absorption band in the region between 1610  $\text{cm}^{-1}$  and 1560  $\text{cm}^{-1}$ , which is due to  $\text{COO}^-$  groups [27] (spectrum 1). The spectrum of PEO (spectrum 2) shows the characteristic bands of  $-\text{CH}_2-$  groups in the region between 2990  $\text{cm}^{-1}$  and 2850  $\text{cm}^{-1}$  [28]. The third spectrum is that of PCL, which shows an absorption band between 1750  $\text{cm}^{-1}$  and 1740  $\text{cm}^{-1}$  due to  $\text{C}=\text{O}$  groups [29]. The spectrum of the polymer coated ENM (spectrum 4), shows the characteristic peaks of the functional groups of the polymers used in membrane production, previously mentioned, therefore indicating that a thin layer of PEO/SA was deposited on the PCL support. Moreover, a

**Table 1**  
Contact angles from the FSM, Nylon, uncoated ENM (PCL support) and PCL coated ENM.

Membranes	Water contact angle
<i>FSM0.45PP</i> – 0.45 $\mu\text{m}$	$85.5^\circ \pm 3.5^\circ$
<i>Nylaflo</i> – 0.22 $\mu\text{m}$	$18.4^\circ \pm 0.1^\circ$
PCL ENM	$104^\circ \pm 7^\circ$
PCL ENMC	$16.8^\circ \pm 2.4^\circ$

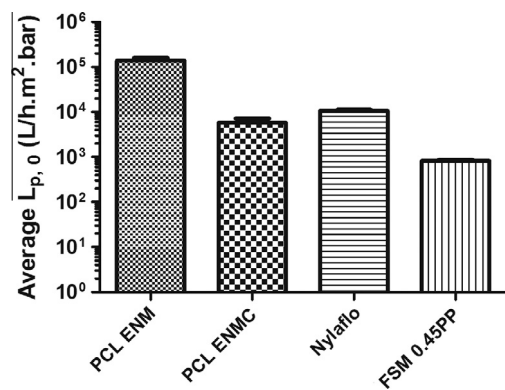


Fig. 6. Water permeability (hydraulic permeability) of the different membranes tested,  $T = 25$  °C, before the filtration tests ( $L_{p,0}$ ).

much higher intensity peak around  $3300\text{ cm}^{-1}$  was observed, due to the over-abundance of  $\text{—OH}$  groups in the coating layer, as previously described in the literature [30,31].

In order to further characterize the surface properties of the membranes, water contact angles were also determined to evaluate the hydrophilicity of the membranes. This is an important property when considering the filtration of suspensions with high organic load; in fact, it is well-known that hydrophilic membranes generally perform better than hydrophobic due to adsorption phenomena [32]. The obtained contact angles are indicated in Table 1. As can be seen, the uncoated PCL membrane presented a high contact angle of  $104^\circ$ , which is indicative of a hydrophobic character. After coating it with PEO/SA the contact angle decreased to  $16.8^\circ$ , which is a very similar value to that of the *Nylaflo* membrane. The contact angle of the *FSM0.45PP* membrane is also very high, although lower than that of the uncoated PCL ENM. Herein, the filtration tests performed with this membrane aimed to check the effect of the pore size on the permeate turbidity and permeability recover after filtration.

### 3.2. Membrane filtration studies

#### 3.2.1. Hydraulic permeability

The results obtained in the permeability tests are summarized in Fig. 6. As can be seen, the coated PCL ENM produced have  $L_{p,0}$  values near  $5000\text{ L/h m}^2\text{ bar}$ , which are of the same order of magnitude of those found for the *Nylaflo* membrane. The hydraulic permeability of the *FSM0.45PP* is clearly lower, which is possibly due to its lower porosity and also its higher hydrophobicity, as suggested by the results obtained from contact angle measurements.

#### 3.2.2. Microfiltration of lysates

After the cell lysis procedure is completed, using the previously described method, a suspension containing a large quantity of precipitates and cell debris is formed, nearly  $2.4\text{ g}$  of suspended solids per gram (wet weight) of cells, as described elsewhere [33]. In respect to solids removal, the coated PCL ENMs and the *Nylaflo* membranes gave identical results. Practically, all solids were removed during the filtration, as can be seen by the turbidity measurements (Table 2). This indicates that both membranes have a similar average pore size. The fact that the uncoated ENMs have a lower solids retention than the coated is in agreement with their higher average

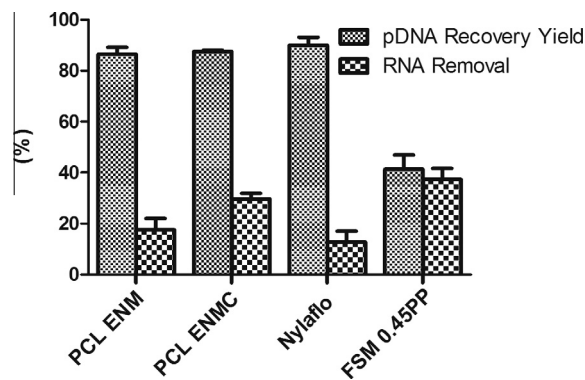


Fig. 7. Filtration yield of the different membranes tested in the filtration of lysates.

fiber diameter, considering that the dimensions of the interstices between fibers becomes smaller as the fiber diameter decreases.

In respect to the process yield, in a previous study, where the same lysis method was used the *Nylaflo* membranes presented high yields for the recovery of pVAX1-lacZ from the obtained lysates [5]. Using both coated and uncoated ENMs, high recovery yields were also obtained herein, as indicated in Fig. 7. In addition, the results also reveal that a significant RNA removal can be achieved using the ENMs, reaching approximately 30% with the PCL coated ENM. It is possible that the structural differences between ENMs and conventional microfiltration membranes can explain the improved selectivity of the ENMs.

With the *FSM0.45PP* membrane the highest RNA removal was found, however, much lower yields are also obtained. The occurrence of severe fouling is likely to be the cause of the higher retention of both pDNA and RNA. In fact, after a few minutes of filtration with this membrane, the permeate pump was unable to impose the predetermined flow of  $0.5\text{ mL/min}$  ( $73\text{ L/h m}^2$ ), which is indicative of the intense fouling. In order to accomplish the filtration, the stirred cell had to be connected to a pressurized nitrogen reservoir containing the diafiltration buffer; the applied pressure on the feed was adjusted to  $0.5\text{ bar}$  and the permeate pump was disconnected. The permeate flux decreased from  $140\text{ L/h m}^2$  to near  $20\text{ L/h m}^2$  by the end of the diafiltration. Fluxes were determined from the volume of permeate collected as a function of time.

The fouling tendency of the different membranes can be better evaluated by comparing the recovery of hydraulic permeability after filtration, i.e., after replacing the lysate suspension inside the cell with water and then, measuring the water permeability (without subjecting the membranes to any cleaning procedure). The ratio  $L_p/L_{p,0}$ , is a measure of the tendency of the membranes to foul; the obtained values are shown in Fig. 8. As can be seen, the coated PCL ENMs recovered almost completely their initial permeability upon filtration of the lysates. This indicates that the produced membranes are highly resistant to fouling by the cell debris and other suspended solids present in the lysates.

The differences between the coated and uncoated ENMs should be also pointed out, with the results clearly showing the importance of the PEO/SA layer in preventing membrane fouling. The decrease in the average fiber size may have contributed to a better performance of the coated membranes, by avoiding the accumulation of solids between the fibers, inside the electrospun films. However, the decisive factor affecting membrane performance is more likely to be the increase in hydrophilicity, as it is suggested

Table 2  
Turbidity of processed lysates (by centrifugation or microfiltration).

Centrifugation <sup>a</sup>	PCL ENM	PCL ENMC	<i>Nylaflo</i>	<i>FSM0.45PP</i>
$0.002 \pm 0.001$	$0.030 \pm 0.001$	$0.0060 \pm 0.0009$	$0.0065 \pm 0.0009$	$0.024 \pm 0.008$

<sup>a</sup> As described in Section 2.2.4.

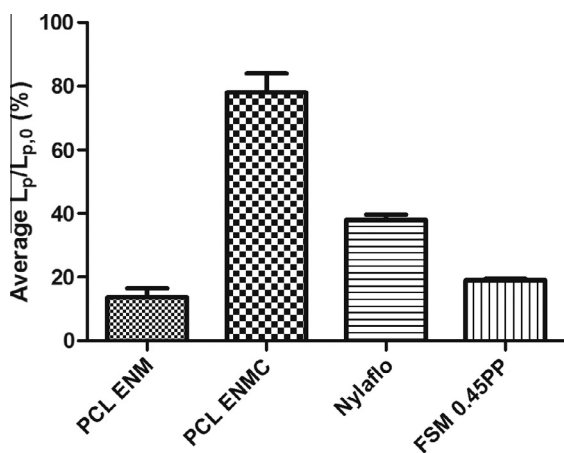


Fig. 8. Permeability recovery of the different membranes tested in the filtration of lysates.

from the fact that both the uncoated ENMs and the *FSM0.45PP* membranes (that had the highest contact angles) present the lowest  $L_p/L_{p,0}$  values.

#### 4. Conclusion

In this work a bi-layer membrane was produced, by deposition of a PEO/SA layer on a PCL support. Both layers were produced by electrospinning. Electrospun nanofibers that have been previously used in a practical and cost-effective way for the production of polymer scaffolds, are shown here to be also suitable to be used as microfiltration membranes, for processing complex suspensions of solids, with high fouling potential (which is the case of cell lysates). The bi-layer arrangement provided both the selectivity and hydrophilicity required for this application. In fact, the experimental results point out that the bi-layer ENM produced can perform, at least, at the same level as commercial microfiltration membranes, showing a comparable selectivity for retaining the suspended solids while allowing the total permeation of the solute of interest (i.e., the plasmid), with an improved selectivity to retain RNA and an even better resistance to fouling. Moreover, the membranes produced are environmentally friendly due to their known biodegradability.

#### Acknowledgments

This work was supported by the Portuguese Foundation for Science and Technology (FCT), (PTDC/EME-TME/103375/2008 and PTDC/EBB-BIO/114320/2009). To Ricardo Fradique for helping in the production of the graphical abstract.

#### References

- [1] G.N.M. Ferreira, Chromatographic approaches in the purification of plasmid DNA for therapy and vaccination, *Chemical Engineering & Technology* 28 (2005) 1285–1294.
- [2] M.A. Liu, DNA vaccines: an historical perspective and view to the future, *Immunological Reviews* 239 (2011) 62–84.
- [3] A. Mountain, Gene therapy: the first decade, *Trends in Biotechnology* 18 (2000) 119–128.
- [4] K.J. Prather, S. Sagar, J. Murphy, M. Chartrain, Industrial scale production of plasmid DNA for vaccine and gene therapy: plasmid design, production, and purification, *Enzyme and Microbial Technology* 33 (2003) 865–883.
- [5] J.C. Nunes, A.M. Morão, C. Nunes, M.T. Pessoa de Amorim, I.C. Escobar, J.A. Queiroz, Plasmid DNA recovery from fermentation broths by a combined process of micro- and ultrafiltration: modeling and application, *Journal of Membrane Science* 415–416 (2012) 24–35.

- [6] N. Ashammakhi, A. Ndreu, Y. Yang, H. Ylikauppila, L. Nikkola, Nanofiber-based scaffolds for tissue engineering, *European Journal of Plastic Surgery* 35 (2012) 135–149.
- [7] Y.J. Kim, M. Ebara, T. Aoyagi, A smart nanofiber web that captures and releases cells, *Angewandte Chemie International Edition* 51 (2012) 10537–10541.
- [8] M. Sumitha, K. Shalumon, V. Sreeja, R. Jayakumar, S.V. Nair, D. Menon, Biocompatible and antibacterial nanofibrous poly ( $\epsilon$ -caprolactone)-nanosilver composite scaffolds for tissue engineering applications, *Journal of Macromolecular Science, Part A* 49 (2012) 131–138.
- [9] Y. Yang, T. Xia, F. Chen, W. Wei, C. Liu, S. He, X. Li, Electrospun fibers with plasmid bFGF polyplex loadings promote skin wound healing in diabetic rats, *Molecular Pharmaceutics* 9 (2011) 48–58.
- [10] M. Scampicchio, A. Bulbarello, A. Arecchi, M.S. Cosio, S. Benedetti, S. Mannino, Electrospun nonwoven nanofibrous membranes for sensors and biosensors, *Electroanalysis* 24 (2012) 719–725.
- [11] H. Wu, L. Hu, M.W. Rowell, D. Kong, J.J. Cha, J.R. McDonough, J. Zhu, Y. Yang, M.D. McGehee, Y. Cui, Electrospun metal nanofiber webs as high-performance transparent electrode, *Nano Letters* 10 (2010) 4242–4248.
- [12] R. Barhate, S. Ramakrishna, Nanofibrous filtering media: filtration problems and solutions from tiny materials, *Journal of Membrane Science* 296 (2007) 1–8.
- [13] A. Cooper, R. Oldinski, H. Ma, J.D. Bryers, M. Zhang, Chitosan-based nanofibrous membranes for antibacterial filter applications (CARBPOL-D-12-01692-R1, August 26, *Carbohydrate Polymers* 92 (2012) 254–259.
- [14] K. Yoon, K. Kim, X. Wang, D. Fang, B.S. Hsiao, B. Chu, High flux ultrafiltration membranes based on electrospun nanofibrous PAN scaffolds and chitosan coating, *Polymer* 47 (2006) 2434–2441.
- [15] N. Bhardwaj, S.C. Kundu, Electrospinning: a fascinating fiber fabrication technique, *Biotechnology Advances* 28 (2010) 325–347.
- [16] R. Gopal, S. Kaur, Z. Ma, C. Chan, S. Ramakrishna, T. Matsuura, Electrospun nanofibrous filtration membrane, *Journal of Membrane Science* 281 (2006) 581–586.
- [17] K.C. Krogman, J.L. Lowery, N.S. Zacharia, G.C. Rutledge, P.T. Hammond, Spraying asymmetry into functional membranes layer-by-layer, *Nature Materials* 8 (2009) 512–518.
- [18] L.A. Bosworth, S. Downes, Physicochemical characterisation of degrading polycaprolactone scaffolds, *Polymer Degradation and Stability* 95 (2010) 2269–2276.
- [19] X. Qin, D. Wu, Effect of different solvents on poly(caprolactone) (PCL) electrospun nonwoven membranes, *Journal of Thermal Analysis and Calorimetry* 107 (2012) 1007–1013.
- [20] J.W. Lu, Y.L. Zhu, Z.X. Guo, P. Hu, J. Yu, Electrospinning of sodium alginate with poly (ethylene oxide), *Polymer* 47 (2006) 8026–8031.
- [21] V. Gaspar, F. Sousa, J. Queiroz, I. Correia, Formulation of chitosan-TTP-pDNA nanocapsules for gene therapy applications, *Nanotechnology* 22 (2010) 015101.
- [22] S.S. Zargarian, V. Haddadi-Asl, A nanofibrous composite scaffold of PCL/hydroxyapatite-chitosan/PVA prepared by electrospinning, *Iran Polymer Journal* 19 (2010) 457–468.
- [23] G. Ma, D. Fang, Y. Liu, X. Zhu, J. Nie, Electrospun sodium alginate/poly (ethylene oxide) core-shell nanofibers scaffolds potential for tissue engineering applications, *Carbohydrate Polymers* 87 (2012) 737–743.
- [24] P. Coimbra, P. Alves, T. Valente, R. Santos, I. Correia, P. Ferreira, Sodium hyaluronate/chitosan polyelectrolyte complex scaffolds for dental pulp regeneration: synthesis and characterization, *International Journal of Biological Macromolecules* 49 (2011) 573–579.
- [25] H.L. Nie, L.M. Zhu, Adsorption of papain with Cibacron Blue F3GA carrying chitosan-coated nylon affinity membranes, *International Journal of Biological Macromolecules* 40 (2007) 261–267.
- [26] A. Bazargan, M. Keyanpour-rad, F. Hesari, M.E. Ganji, A study on the microfiltration behavior of self-supporting electrospun nanofibrous membrane in water using an optical particle counter, *Desalination* 265 (2011) 148–152.
- [27] C. Sartori, D.S. Finch, B. Ralph, K. Gilding, Determination of the cation content of alginate thin films by FTIR spectroscopy, *Polymer* 38 (1997) 43–51.
- [28] S.S. Ojha, D.R. Stevens, T.J. Hoffman, K. Stano, R. Klossner, M.C. Scott, W. Krause, L.I. Clarke, R.E. Gorga, Fabrication and characterization of electrospun chitosan nanofibers formed via templating with polyethylene oxide, *Biomacromolecules* 9 (2008) 2523–2529.
- [29] J. Yang, S.B. Park, H.G. Yoon, Y.M. Huh, S. Haam, Preparation of poly  $\epsilon$ -caprolactone nanoparticles containing magnetite for magnetic drug carrier, *International Journal of Pharmaceutics* 324 (2006) 185–190.
- [30] C.Y. Tang, Y.N. Kwon, J.O. Leckie, Probing the nano- and micro-scales of reverse osmosis membranes—a comprehensive characterization of physicochemical properties of uncoated and coated membranes by XPS, TEM, ATR-FTIR, and streaming potential measurements, *Journal of Membrane Science* 287 (2007) 146–156.
- [31] C.Y. Tang, Y.N. Kwon, J.O. Leckie, Effect of membrane chemistry and coating layer on physicochemical properties of thin film composite polyamide RO and NF membranes: I. FTIR and XPS characterization of polyamide and coating layer chemistry, *Desalination* 242 (2009) 149–167.
- [32] I.S. Chang, S.O. Bag, C.H. Lee, Effects of membrane fouling on solute rejection during membrane filtration of activated sludge, *Process Biochemistry* 36 (2001) 855–860.
- [33] I. Theodossiou, I. Collins, J. Ward, O. Thomas, P. Dunnill, The processing of a plasmid-based gene from *E. coli*. Primary recovery by filtration, *Bioprocess and Biosystems Engineering* 16 (1997) 175–183.